JOURNAL OF MATERIALS SCIENCE 17 (1982) 558–574

Residual stresses in plastics, rapidly cooled from the melt, and their relief by sectioning

N. J. MILLS
Department of Metallurgy and Materials, University of Birmingham, Birmingham, UK

A theory for the residual stresses in tempered glass plates has been adapted for the cooling of plastics, which have temperature dependent thermal properties. The theory was checked against experimental residual stress distributions found in quenched polycarbonate sheet, and against the analytical solution for temperature independent properties. The heat transfer coefficient for quenching polycarbonate from 170° C into iced water was found to lie between 1000 and 4000 W m^{-2} K. It is known that the cutting of thin sections from a sheet relieves the residual stresses, and this is used for transparent plastics to distinguish between orientation and stress bi-refringence. An elastic stress analysis of the sectioning process showed that the section width must be less than 20% of the sheet thickness for the residual stresses to be reduced to 5% of their original values.

1. Introduction

There has been considerable interest recently in the measurement of residual stresses in a variety of polymers including polycarbonate, PC [1, 2], polystyrene, PS [3], polyethylene, PE [4], polypropylene, PP [5], a polyamide [6], and polymethylmethacrylate, PPM [1, 2]. These residual stresses occured as a result of the rapid cooling in the injection moulding or extrusion processes. These are real stresses that act at room temperature, and can be released by cutting up the polymer. They should not be confused with molecular orientation, which is also present, and has been caused by the stresses involved in the flow of a viscoelastic liquid into a mould or through a die. When the flow ceases the molecular orientation begins to relax, but solidification often occurs before this process is complete, and the molecular orientation is frozen in. Although such molecular orientation can be predicted [7] it is not considered in this paper, except as a phenomenon to be separated from stress bi-refringence by suitable sectioning experiments. The object of this paper is to find a suitable theory for the residual stresses that arise as a result of heat flow in one dimension, using the known temperature dependent thermal properties of the polymer.

A number of attempts have been made to predict the stresses that arise due to the tempering of plates of soda-lime–silica glass. In the theory of Aggarwala and Saibel [8] it is assumed that the glass changes from a zero viscosity liquid to an elastic solid when the temperature falls below a certain value, that is approximately equal to the glass transition temperature T_g. In a recent review [9] the modelling of the viscoelastic behaviour of the glass in the transition range was discussed. It was shown that this had to be done with care to produce results that were better than those obtained assuming a sudden transition from an inviscid liquid to an elastic solid. The common feature of the predictions is that the in-plane tensile components of the residual stress vary from a maximum tensile value at the midplane to a maximum compressive value at the surfaces.

Since this type of residual stress distribution has been observed in plastic sheets [1], it is likely that some features of the theories developed for silicate glasses should be applicable for plastics. The experimental determination of residual stresses is a lengthy process, whether it may be by sectioning and bi-refringence measurements [2], by progressively machining away one side of the sheet and monitoring the resulting curvature [1], or by

0022–2461/82/020558–17$3.70/0

interpreting stress relaxation measurements [10], so it would be an advantage to be able to predict the residual stresses that arise as a result of plastics processing.

Knappe [11] has quoted a formula from Timoshenko [12] that describes a parabolic variation of stress with position in a sheet. However reference to Timoshenko shows that the formula is the result of a thermoelastic calculation for a sheet in which the temperature varies parabolically with position. Such a theory cannot explain the existance of residual stresses in a sheet at a uniform temperature. Rigdahl [13] has presented some limited results of residual stress calculations for three-dimensional heat flows in polystyrene using the finite element method. However there do not appear to be any one-dimensional heat flow theories suitable for polymers.

In the present paper, in order to keep the boundary conditions simple, only the thermal tempering of a freely suspended sheet is analysed. However, the results should apply to most extruded profiles of a relatively simple shape, since the melt pressure reduces to atmospheric pressure on leaving an extruder, and cooling is achieved by the use of water baths, without any large axial force on the extrudate. However, in the injection moulding process considerable variations in pressure occur during solidification in the mould. Consequently, both the pressure–volume–temperature relationship of the polymer, and the degree of shape constraint imposed by the mould, need to be included in any analysis of residual stress development. This complicates the analysis, so consideration of injection moulding will be left to a subsequent paper.

When sections from transparent plastic sheet are examined by transmitted polarized light, the interpretation of the bi-refringence measurements is not easy. A recent publication [2] suggested that stress bi-refringence and bi-refringence due to frozen-in molecular orientation could be separated by measuring the bi-refringence before and after cutting thin slices; and that these slices should be less than 1 mm thick (from a sheet initially 4 or 13.5 mm thick). As these recommendations are based only on observed changes in bi-refringence patterns it was thought worthwhile to calculate the stress pattern in a slice taken from a residually stressed plate, using a recently developed boundary element stress analysis technique [14], to see if such slicing would remove the residual stress contributions to bi-refringence.

One major reason for tempering silicate glass sheets is to strengthen them against bending or impact forces, by making it harder for surface cracks to propagate. Although residual stresses are not deliberately introduced into plastic products, it is possible that they would have the same effect. Experiments have been made [15] to see the effect of notching of plastic sheets containing residual stresses, but in interpreting these experiments it was assumed that the cutting of a notch did not disturb the residual stresses. This is an implausible assumption, so calculations were made of the effect of partially sectioning a residual stressed plate, which is equivalent to introducing a crack from the sheet surface.

2. Theory

2.1. Results and limitations of analytic theory

The cooling of an infinite sheet by heat flow in one dimension has been analysed, and analytic solutions given when the sheet has a uniform initial temperature, and there is either a finite or an infinite heat transfer coefficient to a surrounding medium that undergoes a step change in temperature [16]. These analytic expressions have been used [7] to calculate the residual stresses on cooling from an initial temperature that is well above T_s, the temperature at which the viscosity is assumed to increase from zero to an infinite value. For a sheet thickness of $2z_0$(m), a heat transfer coefficient at the sheet surface of h (W m^{-2} K), and a sheet material of thermal conductivity k (W m^{-1} K), the magnitude of the residual stresses depends on the Biot modulus [17] defined by

$$N_{\text{Biot}} = \frac{hz_0}{k}. \tag{1}$$

The in-plane residual stresses, σ_{xx} and σ_{yy}, at a distance z from the mid-plane, see Fig. 1, are given by

$$\sigma_{xx} = \sigma_{yy} = \frac{E\alpha(T_s - T_0)}{1-\nu}\left(1 - \frac{\text{Sin}\,\delta}{\delta} - I_1\right), \tag{2}$$

where E is the Young's modulus, α is the coefficient of thermal expansion for temperature between T_0, the temperature of the surrounding medium, and T_s, and ν is Poisson's ratio. δ is the first root of the equation

$$\delta \tan \delta = N_{\text{Biot}}, \tag{3}$$

and I_1 is the integral

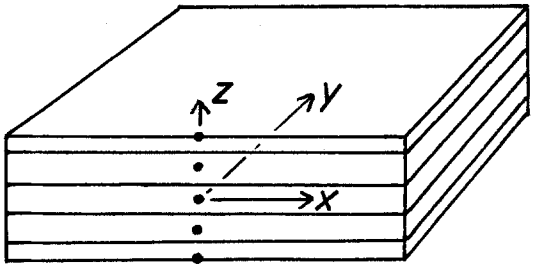

Figure 1 Division of infinite sheet of thickness, $2z_0$, into layers for finite difference heat transfer calculations. Nodal points at which the temperatures are calculated are shown as ○.

$$I_1 = \int_0^{\delta z/z_0} \frac{\text{Sin}\, x\, \text{Sin}\, ½\,(\delta - x)\, \text{Cos}\, ½\,(\delta + x)}{½\,(\delta - x)\, \text{Cos}^2\, x}\, dx \tag{4}$$

The notation has been changed slightly from that used by Aggarwala and Saibel [8], so that it is consistent with the use of the Biot modulus. For values of the Biot modulus $\ll 1$, then the expression in brackets in Equation 2 becomes approximately

$$\frac{\delta^2}{2}\left(\frac{1}{3} - \frac{z^2}{z_0^2}\right) \tag{5}$$

showing that the residual stress varies parabolically with distance. The simple expression 5, cannot be used regardless of the value of N_{Biot}, as was done in [6]. A major limitation of the analytic solution is the assumption that both Young's modulus and the thermal properties are independent of temperature. Consequently, a finite difference method of solution was used to incorporated temperature dependent material parameters. The analytic solution was then used as a check on the validity of the finite difference method. If the initial temperature is only slightly above T_s, then higher roots of Equation 3 should be incorporated in Equation 2.

2.2. Finite difference method of residual stress calculation

When the temperature only varies in one dimension, as in the cooling of an infinite sheet from both sides, a one dimensional finite difference method can be used. Many textbooks [17] explain the basis of the explicit method, and Gardon [18] has used this method for the tempering of glass plates. Fig. 1 shows how the sheet is split into layers of thickness Δz, with the surface layer having a thickness $\Delta z/2$ so that the heat diffusion distances between the 'nodes', at which the temperatures are calculated, are equal. Temperature profiles are only calculated at time intervals Δt, and the temperature after an elapsed time of $(j + 1)\ \Delta t$ is calculated from the temperature profile after $j\Delta t$ using

$$T_{i,j+1} = T_{i,j} + D(T_{i-1,j} + T_{i+1,j} - 2T_{i,j}), \tag{6}$$

where the subscript i refers to the node number, and D is the dimensionless thermal diffusivity given by

$$D = k\Delta t/(\rho c_p \Delta z^2) \tag{7}$$

where ρ is the density, and c_p the specific heat.

At the surface of the sheet, where there is a heat transfer coefficient, h, Equation 6 cannot be used, and instead the new temperature of the first layer is calculated using

$$T_{1,j+1} = 2HT_0 + (1 - 2D - 2H)T_{1,j} + 2DT_{2,j}, \tag{8}$$

where T_0 is the temperature of the external environment, and H is the dimensionless heat transfer coefficient such that

$$H = h\Delta t/(\rho c_p \Delta z). \tag{9}$$

There is a restriction on the magnitude of the time interval, Δt, to ensure that oscillatory solutions do not occur; expressed in terms of H and D the restriction is that

$$D + H \leqslant ½. \tag{10}$$

Temperature dependence of the thermal properties of polymers is particularly marked if there is a glass to liquid transition, or if crystallization occurs in the case of semi-crystalline polymers. This was recognized by Kenig and Kamal [19] who made cooling predictions for cylindrical polyethylene specimens. Temperature dependent constants can be used in Equations 6 and 8 so long as the node temperatures are known i.e. the 'old' temperature is used to find the thermal properties of the layer. Proceeding to the residual stress calculations, a number of further assumptions must be made about the geometrical constraints and the materials properties:

(a) The sheet remains flat during cooling. This will be the case for an infinite sheet cooled equally from both sides, or for an extruded profile, such as a pipe, of symmetric shape. Later calculations

of the effect of sectioning will reveal the size of sheet that is effectively 'infinite'.

(b) The sheet is free to contract in any direction without changing the heat transfer conditions at the surface, and the external pressure remains at atmospheric throughout. External forces in the plane of the sheet are negligible. This will be the case for a freely suspended sheet, or for an extruded profile that is cooled by contact with a water bath.

(c) There is a temperature, T_s, at which the properties of the polymer change from liquid-like to solid-like. For glassy polymers T_s will be just below T_g, for semi-crystalline polymers T_s will be approximately the temperature at which crystallization is complete. Any flow stresses while the polymer is above T_s are negligible, and likewise any viscoelastic effects while the temperature is below T_s can be neglected. (This may be a poor assumption for semi-crystalline polymers).

(d) Once the polymer cools below T_s it becomes a linearly elastic solid, for which the Youngs modulus, E, is a function, $E(T)$, of temperature.

(e) The rate of cooling through T_s does not have a structural effect on the polymer; in particular it does not affect the density at any lower temperature. This is an approximation for glassy polymers since the density does increase slightly for slower cooling rates, and it is known that for silicate glasses that the fictive temperature changes with the rate of cooling, and that this contributes roughly 24% to the residual stresses [20]. For certain crystalline polymers the cooling rate affects the crystal form and/or the degree of crystallinity, and hence the density [6].

(f) For temperatures below T_s, the coefficient of linear expansion, α, is constant.

(g) Although the thermal conductivity, the specific heat and the density can vary with temperature, the heat transfer coefficient is independent of temperature.

It can be deduced from Assumptions c, d and e that the ith layer has a reference length L_i, which is its gauge length in either the x or y-directions when its temperature $= T_s$ and it is stress free. The value of this length for the outmost layer, L_i, is given the value of 1.0. At any lower temperature, when the in-plane residual stress components are $\sigma_{xx} = \sigma_{yy} = \sigma_i$, and the in-plane strain components are $e_{xx} = e_{yy} = e_i$, the gauge length becomes L, given by

$$e_i = \frac{L - L_i}{L_i} = \frac{\sigma_i(1-\nu)}{E_i} + \alpha(T_i - T_s), \quad (11)$$

where E_i denotes the Youngs modulus corresponding to the layer temperature T_i. Since the sheet remains flat, the gauge length, L, of each layer is the same, and the value of L can be found from the condition that there is no external force in the x or y directions

$$\sum_{i=1}^{m} \sigma_i b_i = 0 \quad (12)$$

when m layers are solid, and b_i is the thickness of the ith layer. Substituting for σ_i in Equation 12 gives

$$\frac{1}{1-\nu} \sum_{i=1}^{m} E_i b_i \left[\frac{L}{L_i} - 1 - \alpha(T_i - T_s) \right] = 0 \quad (13)$$

Hence

$$L = \frac{\sum_{i=1}^{m} E_i b_i [1 + \alpha(T_i - T_s)]}{\sum_{i=1}^{m} E_i b_i / L_i}. \quad (14)$$

Every time that the cooling calculation predicts that another layer has cooled below T_s, Equation 14 is used to find L; and the L_i of the newly solidified layer is given this value. When solidification is complete Equations 14 and 11 are used to find the residual stresses at room temperature when all the $T_i = T_{room}$. A brief computer programme, written in FORTRAN, was used to calculate the residual stress distribution.

2.3. Sectioning a sheet that contains residual stresses

The last two sections show that an infinite sheet, which has been cooled by one-dimensional heat flow in the z-direction, may contain a residual stress distribution

$$\sigma_{xx} = \sigma_{yy} = \sigma(z) \qquad \text{for } z_0 > z > -z_0$$

and

$$\sigma_{zz} = \sigma_{xy} = \sigma_{yz} = \sigma_{zx} = 0 \quad (15)$$

where the function $\sigma(z)$ is either determined analytically, or approximated by a set of discrete values $\sigma(z_i)$. If this sheet is sectioned by two parallel planes that are normal to the x-axis, Fig. 2a, the result is a strip of rectangular cross section and infinite extent in the y-direction. On the two new free surfaces ABB'A' and CDD'C'

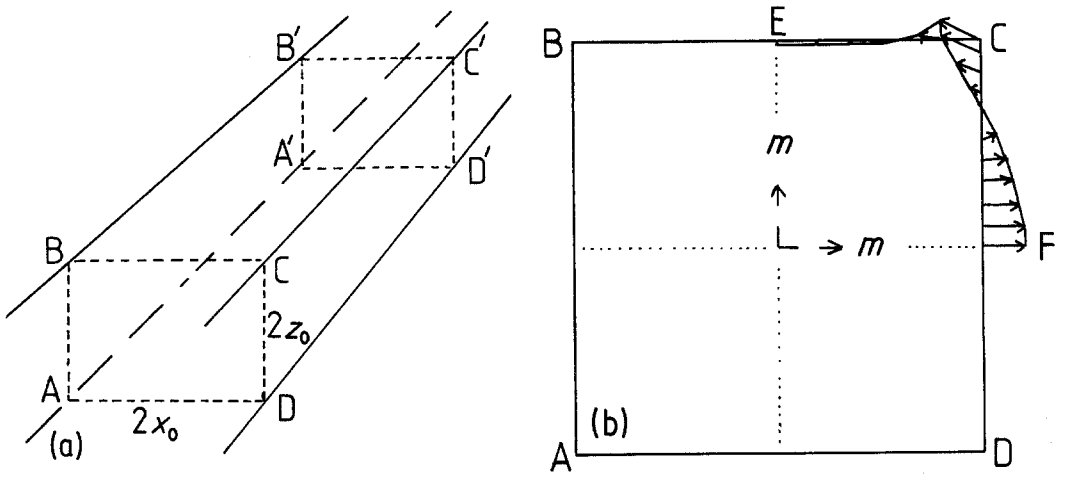

Figure 2 (a) A strip of cross section ABCD, and infinite length, cut from the infinite sheet in Fig. 1. (b) A residually stressed infinite body with imbedded displacement discontinuities that make the boundary ABCD free of normal and shear stress. The magnitude of the discontinuities, exaggerated 40 fold, is shown around ECF, with material overlap being represented by vectors pointing inside the boundary. The mirror planes, m, create image discontinuities that complete the boundary.

the normal and shear stress components σ_{xx} and σ_{xz} are zero. We wish to find the stress distribution in the xz-plane within the strip of cross section ABCD.

The method used to solve this problem is that of boundary elements, each element consisting of a linear array of generalized edge dislocations [14]. However these displacement discontinuities exist in an infinite body, so we must solve a problem that is equivalent to that described above. The infinite body is constructed by bonding together a residually stressed sheet, with stresses given by Equation 15, with two stress free half spaces $z > z_0$ and $z < -z_0$. We are then concerned with a plane strain deformation in the xz-plane of this infinite body see Fig. 2b. In it AB is the intersection with the plane $x = -x_0$, BC is the intertion with the plane $z = z_0$, etc. The n displacement discontinuity elements are arranged around the outside of the boundary ABCD, with the disolcation line running in the y-direction. The magnitudes of the normal and shear components of the displacement discontinuity at the centre of each element are chosen so that the average normal stress and shear stress on each element boundary is zero. This is done by solving a set of $2n$ simultaneous equations. Since the boundary stresses on ABCD in the infinite body in Fig. 2b are now the same as those on the boundary ABCD of the infinite strip in Fig. 2a, the stress field within ABCD will be the same in the two cases. Therefore we can use the boundary element method to find the stress distribution within the strip ABCD.

The calculation is simplified by noting that two perpendicular mirror symmetry planes exist in Fig. 2b, so that the unknown displacement discontinuities on the boundary ECF have their images in the other three quadrants. Along CF the elements are centred on the nodal positions used in the finite difference cooling calculation, so that $\sigma(z_i)$ represents the residual stress at the centre of each element. The calculations were made with the assumption of plane strain deformation, so stresses $\sigma_{yy} = -\nu(\sigma_{xx} + \sigma_{zz})$ also occur. The stress field inside a quadrant of the boundary ABCD was presented graphically using the CUGHOST graphics package developed by UKAEA Culham Laboratory. Isochromatic contour maps of the maximum shear stress in the xz-plane, and the direction and magnitude of the principal stresses were presented. The stress field in the xz-plane will be the same regardless of whether plane strain or plane stress conditions apply, but the displacement fields differ. If a slice of thickness $2y_0$ is taken from the strip in Fig. 2a, and if $y_0 \ll z_0$ and $y_0 \ll x_0$ (see Fig. 3) then plane stress conditions $\sigma_{yy} = \sigma_{yz} = \sigma_{yx} = 0$ prevail. Such slices have been used for photoelastic observation, and the isochromatic patterns within them can still be compared with those predicted from the plane strain analysis of Fig. 2b.

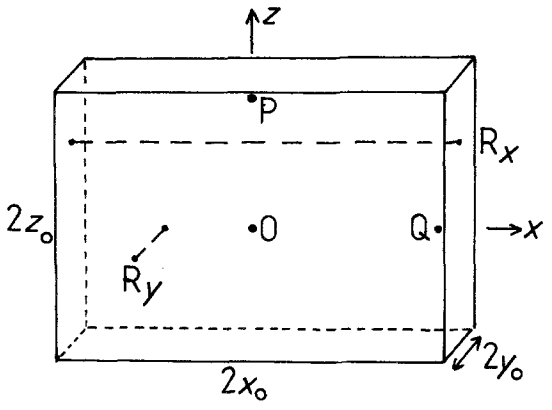

Figure 3 A slice of thickness, $2y_0$, cut from the strip shown in Fig. 2a. The dashed lines are the light paths through the strip for the phase retardation measurements. The stress components at points O, P and Q are tabulated in Table I.

2.4. Partially sectioning a residually stressed sheet

If a cut or a crack only runs part of the way through a sheet of residually stressed material then the boundary value problem is solved in a slightly different way to that described in the previous section. It is necessary to use a result described in Section 3.4, that the effect of completely cutting through a residually stressed sheet does not extend more that 2.5 times the sheet thickness away from the cut. Fig. 4 shows how the problem is modelled in a infinite body that contains the residual stress distribution of Equation 15. Boundary elements

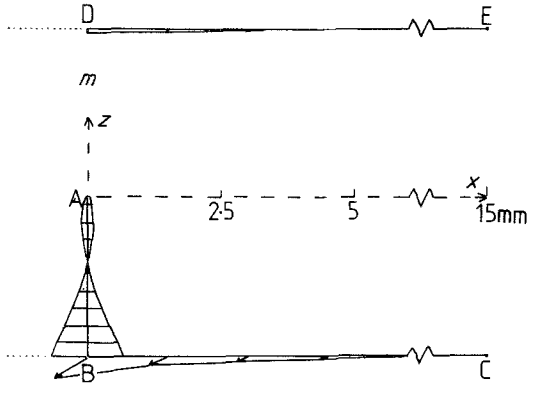

Figure 4 Modelling of a surface crack in a residually stressed sheet. Displacement discontinuities are imbedded along ABC and DE in an infinite residually stressed body, so that these boundaries are free of normal and shear stress. The displacement discontinuity magnitudes, exaggerated 40 fold are shown for the case of a 3 mm crack in a 6.15 mm thick PC sheet. (Note that the crack faces overlap near B.)

extend along BC and DE to a distance $5z_0$ from the crack, and these are mirrored in the plane BD. Elements in which the normal displacement discontinuity varies linearly are used along BA, except that the last element is a crack tip element in which the normal displacement discontinuity varies as the square root of the distance from A. When the boundary value problem is solved the opening of this crack tip element can be used to calculate the stress intensity factor, K_I, at the crack tip [14]. The length, a, of the boundary AB was increased incrementally and the value of K_I was calculated for each length, so that the relationship between K_I and a could be evaluated. If the toughness of the material is known this relationship can then be used to predict the possibility of crack growth. When the isochromatic fringe pattern was predicted for the interior of the region CBDE this confirmed that the effects of the crack were negligible at a distance $x = 5z_0$ from the crack.

2.5. Bi-refringence measurements

Consider a thin slice of plastic such as that shown in Fig. 3. The thickness, $2y_0$ of the slice is sufficiently small so that plane stress conditions exist in the xz-plane. The interpretation of bi-refringence measurements depends on the direction of the light. The simplest case is when the light passes in the y-direction, since the stresses σ_{xx}, σ_{xz} and σ_{zz} do not vary in the y-direction, nor do the principal stresses σ_1 and σ_2 calculated from them. The Wertheim law [21] for a elastic body can be used

$$R_y = C(\sigma_1 - \sigma_2)\,2y_0 \qquad (16)$$

where R_y is the retardation measured in metres, of a ray polarized in the 2-direction compared with a ray polarized in the 1-direction, and C is the stress optical coefficient.

The bi-refringence, $\Delta n = n_1 - n_2$, where n_1 and n_2 are the refractive indices in the 1 and 2 directions, is then given by $\Delta n = R_y/2y_0$.

If the light passes in the x-direction through the slice, the interpretation is more complex, because the stress state varies along the light path. The "secondary principal stresses" at any point for a light ray in the x-direction are calculated from the stress components σ_{yy}, σ_{zz} and σ_{zy} in the plane of which x is the normal. For such a thin slice the σ_{yy} and σ_{zy} stress components are zero, and the secondary principal directions are constant, namely the y and z-axes. Equation 16 is replaced

by the integral Wertheim law, x_0

$$R_x = C \int_{-x_0}^{x_0} (\sigma_{yy} - \sigma_{zz})\, dx. \qquad (17)$$

This can be simplified because (a) $\sigma_{yy} = 0$ under plane stress conditions, and (b) there are no external forces, F_z, on the slice in the z-direction, so the force equilibrium of any section perpendicular to the z-axis gives

$$F_z = 2y_0 \int_{-x_0}^{x_0} \sigma_{zz}\, dx = 0. \qquad (18)$$

Hence, for such a slice $R_x = 0$. A similar arguement will show that the retardation R_z, of any ray travelling in the z-direction through the slice shown in Fig. 3 is zero.

The above arguments are purely for stress bi-refringence caused by residual stresses. If there is further bi-refringence caused by frozen-in molecular orientation, this will not be affected by the cutting of thin sections, and R_x and R_z will be non-zero.

3. Results

3.1. Comparison of the finite difference calculations for constant thermal properties with the analytic theory

Initially the thermal properties of the polymer were assumed to be temperature independent. This should enable calculations for differing values of the heat transfer coefficient, thermal conductivity and sheet thickness to be represented in terms of the non-dimensional Biot modulus. Similarly the magnitude of the residual stress can be normalized by dividing by σ^*, where

$$\sigma^* = E\alpha(T_s - T_0)/(1-\nu). \qquad (19)$$

σ^* combines the elastic properties and thermal expansivity of the material and the solidification and bath temperature that occur in Equation 2. However the finite difference calculations did not use a direct input of N_{Biot} to calculate σ_i/σ^*; instead values appropriate for possible quenching experiments on polycarbonate sheet were used, and it was checked that the results of varying the sheet thickness, $2z_0$, the heat transfer coefficient, h, and the bath temperature, T_0, gave results that superimoposed on a graph of σ_i/σ^* against N_{Biot}. Use of realistic parameters for polycarbonate also allow the predicted residual stresses to be compared with the known yield stress of this material.

At 20° C PC has a thermal conductivity of $0.21\,\text{W m}^{-1}\,\text{K}$, the product of the density and specific heat is $1.42\,\text{MJ m}^{-3}\,\text{K}$, so the thermal diffusivity is $0.15\,\text{mm}^2\,\text{s}^{-1}$. These properties were assumed to be the same at all other temperatures. The Young's modulus of PC decreases only slightly with temperature, so the actual variation was used in the finite difference calculation. A graph of $\ln E$ against temperature can be approximated by straight line segments passing through $2.2\,\text{GN m}^{-2}$ at 20° C, $2.0\,\text{GN m}^{-2}$ at 85° C and $1.75\,\text{GN m}^{-2}$ at 142° C. A Poisson's ratio of 0.4 was used. The solidification temperature used was $T_s = 142°$ C, which is a few degrees below the usually reported T_g of 145° C. It was found that the initial polymer temperature has little effect on the residual stress results so long as it exceeded $T_s + 20°$ C, and the value of the Biot modulus was not excessively high. To be certain that it had no influence on the results an initial temperature of 300° C was used. When the temperature of the environmental bath was 20° C, and room temperature was also assumed to be 20° C, and the linear thermal expansion coefficient, $\alpha = 6.5 \times 10^{-5}\,°\,\text{C}^{-1}$, the value of $\sigma^* = 29.1\,\text{MN m}^{-2}$. The finite difference model only calculates the average residual stresses in each layer; consequently the number of layers must be increased to get a good representation of the residual stress at the outer surface of the sheet, where the stress varies most rapidly. Table I shows how the stresses in the central and surface layers vary as the number of layers increase, for the case of $N_{\text{Biot}} = 10$ (corresponding to $h = 1050\,\text{W m}^{-2}\,\text{K}$ and $z_0 = 2\,\text{mm}$) and $\sigma^* = 29.1\,\text{MN m}^{-2}$.

It is clear that increasing the number of layers beyond 30 hardly changes the calculated stress at the sheet surface. The computations were therefore made for 20 or 30 layers in the half thickness. Fig. 5 shows how the residual stresses vary with the Biot modulus, for the same conditions used for Table I. It shows that the 20 layer finite difference model predicts central residual stresses that are in excellent agreement with Equation 2, and surface residual stresses that are within 11% of Equation 2 for $N_{\text{Biot}} \leqslant 20$. Equation 2 becomes inaccurate for high values of the Biot modulus since additional roots of Equation 3 will be necessary to predict the surface temperature accurately at short times. Consequently the finite difference method can be used with confidence regardless of whether or not the thermal properties of the polymer are temperature independent. Note that the deviation

TABLE I Variation in residual stresses with number of layers used in the finite difference calculation

No. of layers in half the sheet	Central layer stress MN m^{-2}	Surface layer stress MN m^{-2}	Computation time (sec)
11	8.81	−28.99	0.8
20	8.78	−30.43	2.1
30	8.79	−31.01	4.6
37	8.78	−31.15	7.5
Analytic result, Equation 2	8.94	−32.67	

between the surface compressive stress, and twice the central tensile stress which occurs for $N_{Biot} \geqslant 1$, means that the simple parabolic stress distribution of Equation 5 will give erronious predictions.

3.2. Comparison of predictions with published residual stress distributions in glassy polycarbonate

So and Broutman [1] reported residual stress distributions for 6.35 and 3.18 mm thick PC sheets that have been quenched from 150° C into iced water at 1° C. Before being able to predict the residual stresses resulting from such an experiment, it is necessary to have values of the thermal diffusivity of PC, and of the heat transfer coefficient. Berlot [22] has determined the thermal diffusivity at a function of temperature, and the values, at least up to 140° C have been confirmed to within 15%, by calculations from published data on the specific volume [23], specific heat [24], and thermal conductivity [25]. Fig. 6 shows how the thermal diffusivity, and the heat capacity ρC_p vary with temperature; note that the data has been fitted by a number of straight line segments to aid interpolation. The heat transfer coefficient for the quenching of a PC plate from 120° C into iced water was determined by embedding two 0.4 mm diameter thermocouple wires into a 13 mm thick PC plate of area 50 × 50 mm [26]. The plate was made by compression moulding pieces of extruded PC sheet of the appropriate thickness together, with the thermocouple wires lying parallel to the surface to minimize errors due to conduction down the wires. The depths of the thermocouples from the surface were checked by sectioning the sheet after the experiment; they were 0.8 mm from the surface, and at the mid-section. The recorded thermocouple voltages

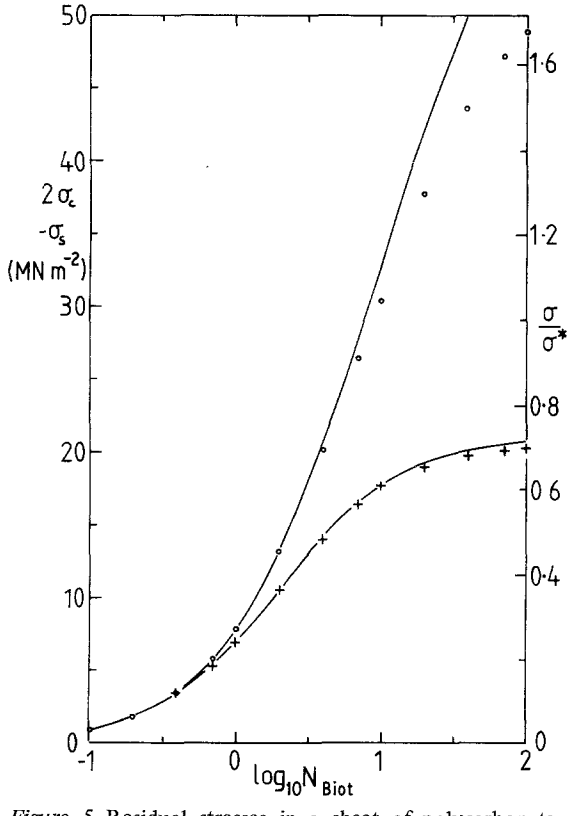

Figure 5 Residual stresses in a sheet of polycarbonate quenched from 300 to 20° C against the Biot modulus. (o) is the surface compressive stress, and (+) is twice the central tensile stress. The solid lines are the analytical solutions using Equation 2. The right hand scale has been normalized using σ^* of Equation 19.

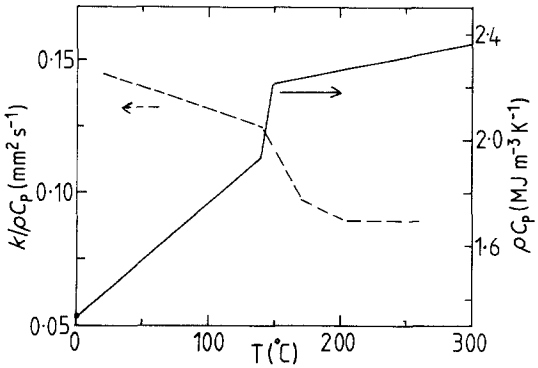

Figure 6 Variation with temperature of the thermal diffusivity and heat capacity per unit volume for polycarbonate.

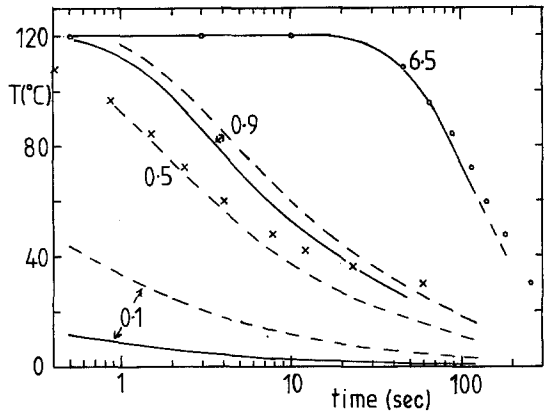

Figure 7 Cooling curves for a 13.1 mm polycarbonate plate, (o) is for the central thermocouple, and (x) the thermocouple 0.8 mm below the surface. The dashed and solid lines are the predictions for heat transfer coefficients of 1000 and 4000 W m^{-2} K respectively, for the depths indicated.

against time in the quenching experiment, were converted to temperatures, and then compared with the predictions of the finite difference calculations, using 30 layers for the sheet half thickness. The temperature dependence of the thermal diffusivity from Fig. 6 was used, and the value of the heat transfer coefficient was varied to get the best agreement with experiment. Fig. 7 shows the experimental points and predictions for three parts of the sheet for $h = 1000$ and $h = 4000$ W m^{-2} K. First note that the temperature of the 0.12 mm thick surface falls to below 9° C in 1 sec for $h = 4000$, so there is little point in increasing h above this value for a 13 mm sheet. The temperature results for the 0.8 mm deep thermocouple fall just below the predictions for the 0.9 mm deep layer for $h = 4000$ W m^{-2} K. There is a very strong temperature gradient in the outer 1 mm of the sheet, so the uncertainty in the effective thermocouple position of ±0.3 mm makes the estimation of the h value imprecise. At the mid-point of the sheet the predicted temperatures for $h = 1000$ or 4000 W m^{-2} K are practically identical. Hence any measurements at this point are largely a check on the thermal diffusivity of the PC; the close agreement with the predictions confirms the diffusivity data of Fig. 6.

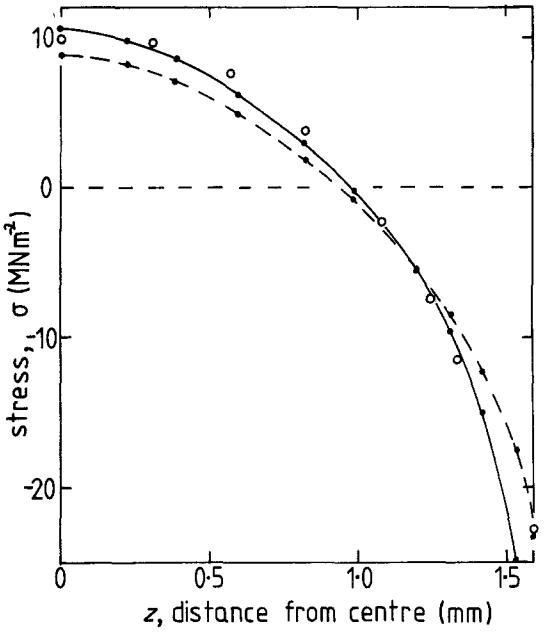

Figure 8 A plot of residual stress against distance from the centre of the sheet for 3.18 mm PC quenched from 150 to 0° C. The residual stress results of So and Broutman are as shown on open circles. The dashed and solid lines are the predictions for $h = 1000$ and 4000 W m^{-2} K respectively for the 20 layer model.

The values of the heat transfer coefficient, and the thermal diffusivity data of Fig. 6 were then used to predict the residual stresses in 3.18 and 6.35 mm thick PC sheet quenched from 150° C to 0° C. Fig. 8 shows the comparison between the results of So and Broutman for the 3 mm sheet (they estimate the errors in the stresses to be 10 to 15%; this is largely due to scatter in the graph of the beam curvature against the thickness milled away), and the predictions for a solidification temperature of $T_s = 142$° C. The predicted residual stress variation for $h = 4000$ W m^{-2} K gives the best agreement with experiment, though the value in the outmost 0.027 mm thick layer at −40 MN m^{-2} is larger than the experimental value of −22.8 MN m^{-2}. Thus there is some doubt about the predicted values within 0.1 mm of the surface. The experimental results of So and Broutman for the 6.35 thick sheet are almost identical with the 3.18 mm sheet results; if anything the stresses are about 10% smaller at the surface. This proves to be a good check on the

TABLE II Predicted mid-thickness residual stresses (MN m^{-2}) in PC quenched from 150 to 0° C

Sheet thickness mm	Residual stresses (MN m^{-2})		
	h* = 4000	h = 1000	h = 200
6.35	10.8	9.9	6.4
3.18	10.5	8.8	4.5

*h in W m^{-2} K.

magnitude of the heat transfer coefficient, as is shown in Table II, where the predicted tensile residual stresses at the centre of various sheet thicknesses are calculated for a range of heat transfer coefficients, for quenching PC from 150° C to 0° C, using $T_s = 142°$ C.

Saffell and Windle [2] have recently published information on the heat transfer coefficient and the residual stresses in the quenching of PMMA and PC sheets. It was hoped to use their data as a further check on the theory. However, a number of mistakes in their analysis make their results questionable. In Fig. 1 of their paper they refer to an experimental cooling curve for the midplane of a 2 mm PMMA sheet cooled by contact with copper sheets at −145° C, as being "fitted with the calculated error function curve for a ratio of surface conductance (h) to the bulk conductivity (k) of 10". "Surface conductance" is the term of Carslaw and Jaeger [16] for the heat transfer coefficient, and the term "error function" infers that they are using the solution for the surface cooling of a semi-infinite body. By checking with Carslaw and Jaeger ([16] page 123 Fig. 17 and page 124 Fig. 18), it is apparent that they have used the correct analytical solution for the sheet of thickness $2e$, cooled on both sides, and that the curves that Saffell and Windle plot are for the dimensionless parameter $L = 1$ ($L = he/k$, i.e. the Biot modulus). Therefore h/k is not dimensionless as Saffell and Windle imply, but has the value 10 cm^{-1} for their sheet of $e = 0.1$ cm. Consequently for PMMA which has a thermal conductivity of 0.2 $W m^{-2} K$ the heat transfer coefficient to copper plates is 200 and not 2.0 $W m^{-2} K$.

Saffell and Windle give graphs of the variation of bi-refringence with distance from the sheet surface for 4 mm PC sheet quenched from 180° C into water at 20° C both before (Fig. 6 of [2]) and after (Fig. 9 of [2]) corrections for residual orientational bi-refringence. These graphs are labelled on the vertical axes both with the bi-refringence Δn and the difference $\sigma_x - \sigma_z$ in the principal stress (this should read $\sigma_y - \sigma_z$!). However the scales have changed between the two figures, and the ratio of the scales, which gives the stress optical coefficient of Equation 14, is 32 Brewsters in Fig. 6 and 108 Br in Fig. 9, whereas the caption of Fig. 6 quotes it as being 1.3×10^{10} Br (1 Brewster = $10^{-12} m^2 N^{-1}$ so I think this means $C = 10^{12}/1.3 \times 10^{10} = 77$ Br). Consequently it is not clear whether the surface residual stress is roughly $-40 MN m^{-2}$ or $-16 MN m^{-2}$. Because of this doubt, some of the quenching experiments were repeated – see Section 3.6.

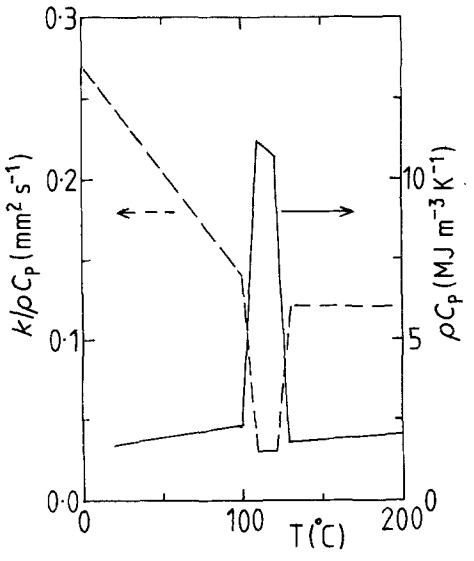

Figure 9 Variation with temperature of the thermal diffusivity and heat capacity per unit volume for HDPE.

3.3. Residual stress predictions for semi-crystalline polyethylene

The semi-crystalline polymer for which the best thermal data exists is polyethylene. However there are no published residual stress data for sheet quenching experiments on PE. Consequently the only comparison with experimental results possible was that for the injection moulding of a high density polyethylene, of a kind that could be subsequently cross linked by moisture [4].

The thermal diffusivity of high density polyethylene (HDPE) has been measured by Hands [27], while the polymer temperature was being increased. Measurement of the specific heat of such a polyethylene during heating and cooling cycles was carried out with a Perkin Elmer DSC-II by courtesy of Dr. J. N. Hay of the Chemistry Department, Birmingham University). This reveals that the specific heat peak due to melting on heating appears as a peak due to crystallization on cooling at a 20 to 30° C lower temperature. Hence the thermal diffusivity for cooling HDPE was estimated from the data of Hands using this temperature shift, and is shown in Fig. 9, together with variation in heat capacity with temperature. The variation in the Young's modulus of HDPE with temperature is far more marked than is the

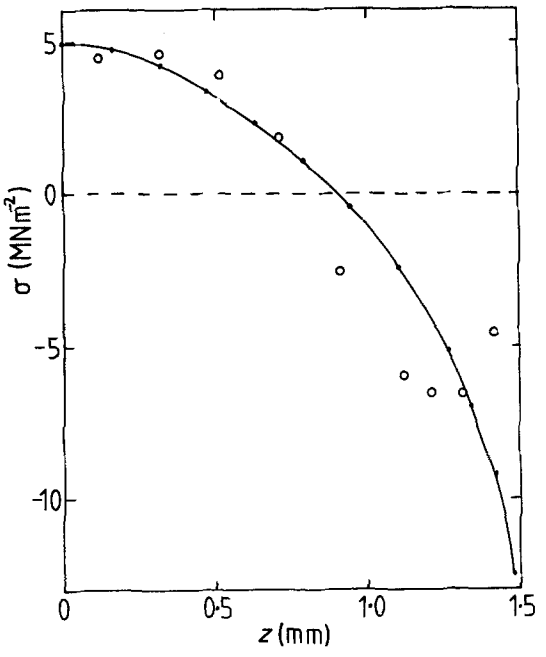

Figure 10 The residual stress for injection moulded HDPE against z. The results of Coxon and White are shown as open circles. The solid lines is the prediction of the 20 layer model for $h = 1000\,W\,m^{-2}\,K$ and $T_s = 110°\,C$.

case for PC, so data from Krigbaum [28] for the 40 sec creep modulus was used, the values being $0.9\,GN\,m^{-2}$ at 20° C and $0.134\,GN\,m^{-2}$ at 95° C, when the data is plotted as ln E against temperature there is an almost linear variation between these limits.

Fig. 10 shows the predicted variation of residual stress in a 3 mm HDPE sheet cooled from 150° C with a surface heat transfer coefficient of $1000\,W\,m^{-2}\,K$. The stresses are smaller than in the PC calculation of Fig. 8, but then so is the yield stress of HDPE i.e. about $25\,MN\,m^{-2}$ at 20° C. The data of Coxon and White [4] using layer removal techniques on injection moulded 3 mm thick bars is also shown. It provides a rough check on the magnitude of the predicted stresses, and shows that the pattern of residual stress variation in injection moulded bars is more complex than in quenched sheets, presumably because of the feeding of the partially solidified moulding; the pressure variations during this process, and the density changes due to crystallization.

Because polyethlene has strongly temperature dependent thermal properties and elastic modulus, it is useful to compare the effect of ignoring one or the other of these temperature dependences and using the 20° C values. Table III shows the predicted central and surface residual stresses under three sets sets of assumptions.

Ignoring all temperature dependences, or using the analytical theory with $N_{Biot} = 3.6$ and $\sigma^* = 17.6\,MN\,m^{-2}$, leads to an error of 17% at the centre of the sheet, and rather less at the sheet surface. The reduction in stress values in the second row compared with the first row is explicable in terms of the colder, and hence stiffer, surface layers resisting the contraction of the other solid layers, and hence increasing the values of the reference lengths L_i of the next layers to solidify. The larger stresses in the third row compared with the second row are a result of the lower average thermal diffusivity in the temperature dependent case, and hence the larger effective value of the Biot modulus.

The conclusions from the comparisons in Table III are that the $E(T)$ correction partially compensates for the variation in thermal diffusivity, and that if an average value of thermal diffusivity for the temperature range of interest were used with the constant properties calculation, the overall error should be less than 10%.

3.4. The effects of sectioning a residually stressed sheet

Calculations of the stress distribution in sections, using the method of Section 2.3, were made both for predicted residual stress distributions and experimentally measured residual stress distributions. Since the results were almost identical, the experimental stress distribution results are

TABLE III Predicted residual stresses in a 3 mm thick polyethylene sheet quenched from 150° C to 20° C for $h = 1000\,W\,m^{-2}\,K$

Conditions		Residual Stresses ($MN\,m^{-2}$)		Solidification time (sec)
$E(T)$	$k(T)\,\rho C_p(T)$	Surface	Centre	
Constant	Constant	−11.1	4.1	3.4
Variable	Constant	−10.8	3.9	3.4
Variable	Variable	−12.5	4.9	13.1

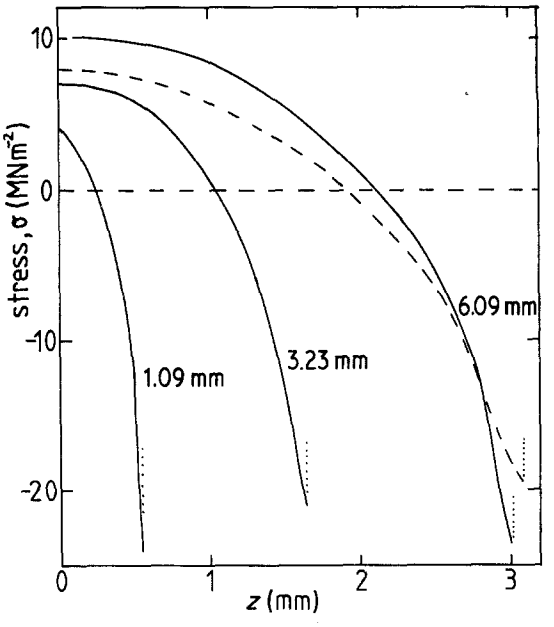

Figure 11 Residual stress variation calculated from bi-refringence measurements on PC sheets quenched from 170° C into iced water. Solid lines represent sheets 1.09 mm, 3.23 mm and 6.09 mm thick. —·—·— represents a 6.15 mm PC sheet quenched from 160 to 0° C.

presented, since they can be compared with photoelastic photographs of sections. The experimental results were for an "infinite" sheet of PC 6.13 mm thick, that was quenched from 160° C into iced water. The calculation of the residual stress distribution from bi-refringence measurements is described in Section 3.6, and Fig. 11 shows the residual stress variation. The central tensile stress was $7.9\,\mathrm{MN\,m^{-2}}$, and the surface compressive stress was $-19.5\,\mathrm{MN\,m^{-2}}$.

Calculations were made for a range of values of the section half width to the sheet half thickness x_0/z_0 (Fig. 3), and the stress components at certain key points are presented in Table IV.

In order to relieve the residual stresses to less than 5% of their values in an infinite sheet, Table IV shows that the section thickness must be $\leqslant 20\%$ of the sheet thickness. (The apparently slightly higher values when $x_0/z_0 = 0.1$ are an artefact due to the boundary elements becoming too close to each other). A thin section with $x_0/z_0 \leqslant 0.2$ will only relieve the σ_{xx} stress components, it will also be necessary for y_0/z_0 to be $\leqslant 0.2$ for σ_{yy} to be relieved. However, such a tall thin section would have low photoelastic sensitivity because of the short light path. The argument in Section 2.5 that the optical retardation due to residual stresses $R_x = 0$, for a thin slice with $y_0 \ll z_0$, regardless of the value of x_0, can be used to design a more useful section shape. Table IV shows that the condition $y_0 \ll z_0$ means effectively that $y_0 \leqslant 0.2 z_0$, so a section obeying this condition, and of sufficient optical path length, $2x_0$, to give adequate sensitivity, can be used to measure the retardation, R_x, and hence the molecular orientation contribution to the bi-refringence.

Table IV also enables us to determine the length of plate that is effectively an infinite sheet. It can be seen that a section with $x_0 \gg 5z_0$ will have at its mid plane, $x = 0$, a fully developed maximum shear stress pattern (Columns 4 and 6 in the table). This does not mean that a plate with $x_0 = y_0 = 5z_0$ can be quenched and thereby contain a fully developed residual stress field at $x = y = 0$, because we have not considered the effect of heat flow in the x or y directions. However by examining by polarized light a plate with $x_0/z_0 \simeq 15$ it is observed that the end effects due to two dimensional heat flow do not extend into the central third of the plate, so if the central third was cut from such a plate it would still contain a fully developed residual stress profile at $x = 0$.

The case of $x_0/z_0 = 5$ is worth examining in more detail, as Saffell and Windle [2] have esti-

TABLE IV Stress components in sections, normalized with respect to residual stresses in an infinite sheet

Section shape	Tensile stress components at the origin		Maximum shear stress at the point (x,z)		
x_0/z_0	$\frac{\sigma_{xx}}{\sigma^{\infty}_{xx}(0)}$	$\frac{\sigma_{zz}}{\sigma^{\infty}_{xx}(0)}$	$\frac{\tau(0,0)}{\tau^{\infty}(0)}$	$\frac{\tau(x_0,0)}{\tau^{\infty}(0)}$	$\frac{\tau(0,z_0)}{\tau^{\infty}(z_0)}$
∞	1.00	0.00	1.00	-	1.00
5.0	0.95	0.00	0.95	1.22	1.02
2.0	0.92	0.09	0.83	1.24	1.01
1.0	0.37	0.44	0.07	1.12	0.69
0.5	−0.01	0.24	0.25	0.38	0.29
0.2	0.00	0.05	0.05	0.00	0.03
0.1	0.00	0.04	0.04	0.06	0.10

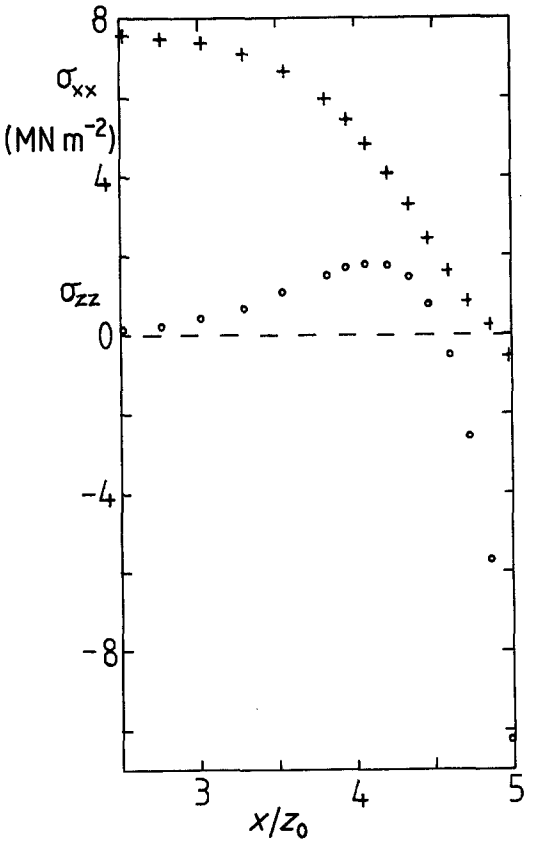

Figure 12 Predicted principal stress variation along the $z = 0$ midplane of a sheet section cut from a 6 mm PC sheet, having a length to thickness ratio of 5, that has been quenched from 160 to 0° C. + represents σ_{xx} and ○ represents σ_{zz}.

mated the residual stress variation in such a section (their Fig. 3). Fig. 12 shows that they are correct in attributing the peak in τ_{max} at the centre of the cut plane to the compressive peak in σ_{zz} at the cut surface, but they are incorrect in assuming this is balanced by a uniform tensile σ_{zz} over the central 80% of the section. Fig. 12 shows there is a tensile peak in the through thickness stress, σ_{zz} at about z_0 from the cut surface, but that this stress component decays to a zero value at the centre of the section.

In a square section with $x_0 = z_0$ a complex stress pattern develops, with a biaxial tension at the origin and peak compressive stress components at the midpoints of each face (Fig. 13a). The overall stress level is of the order of 50% of the infinite sheet case.

3.5. Partially sectioning a residually stressed sheet

The analysis described in Section 2.4 was used to see the effect of partially sectioning a sheet. The residual stress data was for temperature independent thermal properties, $N_{Biot} = 13.3$ and $\sigma^* = 31.5\,MN\,m^{-2}$, and the sheet was taken to be 6.13 mm thick. The first thing to note is that if a sheet is sectioned half way through, the cut ending at $z = 0$ (Fig. 4), the result is not to relieve the stresses in half the sheet, and leave the stresses in the other half untouched. This is because the original residual stresses on the uncut half $z > 0$

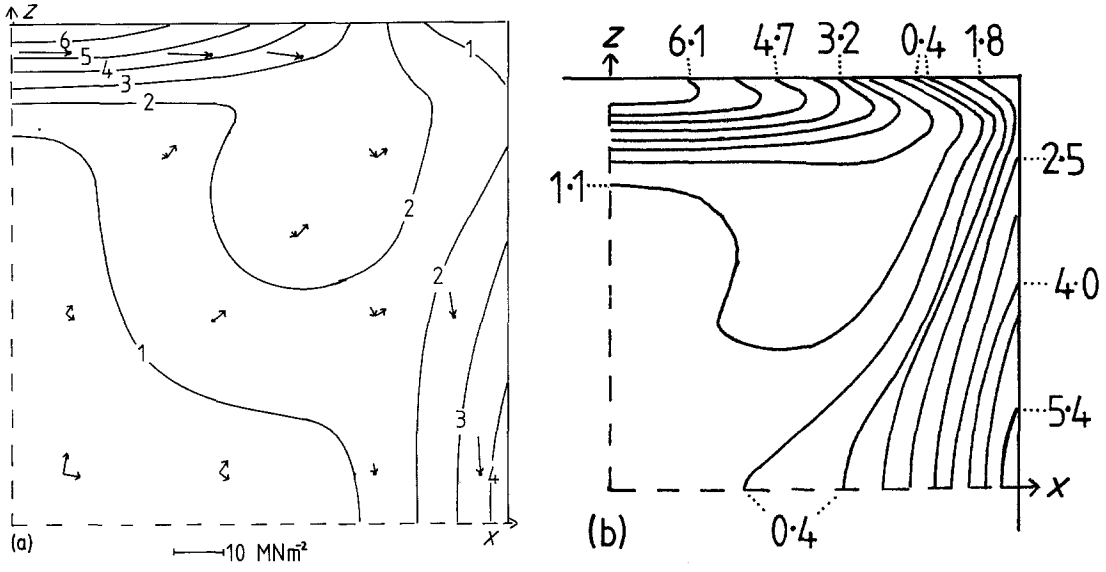

Figure 13 Isochromatic (maximum shear stress) patterns in a square section cut from the same PC sheet as in Fig. 12, the vectors at selected points represent the principal stresses on the scale shown. (a) predicted pattern (b) The observed isochromatic pattern. In both cases the isochromatic contours levels are labelled in MN m^{-2}.

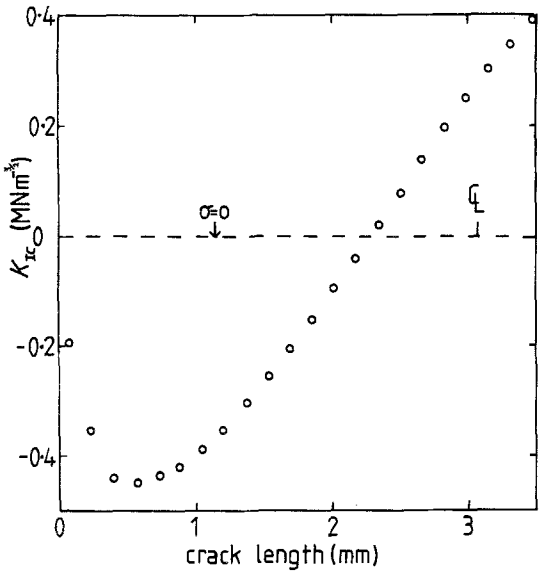

Figure 14 Predicted variation in the stress intensity factor, K_I, of a crack growing from the surface through a 6.15 mm thick PC sheet quenched from 160 to 0° C.

have a net bending moment about the y-axis. Therefore cutting the sheet must modify the residual stress distribution. Since partially sectioning the sheet is of little quantitative use in determing the residual stresses by photoelastic means, no predicted stress distributions have been presented. However, as a crack is a special case of a cut of negligible thickness, it was felt worthwhile to present a fracture mechanics analysis of crack growth through a residually stressed sheet. Fig. 14 shows how the value of K_I varies with the crack length for the 6.13 mm PC sheet modelled. The K_I values are initially negative; in the mathematical model this is achieved by the crack faces overlapping each other, but in reality the crack faces would press on each other, and they would no longer be stress free. If some external tensile or bending load was also applied to the sheet, and this caused a positive K_I value at the crack tip in a sheet that did not contain residual stresses, then the total effect of such a load on the residually stressed sheet would be to cause a stress intensity factor at the crack tip of K_I (external) + K_I (residual stresses). Since this total K_I would determine whether or not the crack should grow, using the fracture mechanics criterion $K_I \geqslant K_{IC}$ where K_{IC} is the critical stress intensity factor of the material, then the effect of the residual stresses is initially to make crack growth less likely.

The K_I value remains negative after the crack has grown past the z-co-ordinate where the residual stresses become tensile in the uncracked sheet. The minimum K_{IC} of $-0.4\,MN\,m^{-1.5}$ in Fig. 14 should be compared with the K_{IC} of about $2.2\,MN\,m^{-1.5}$ for rapid plane strain fracture in monotonically loaded PC, and the threshold ΔK for fatigue crack growth of about $0.9\,MN\,m^{-1.5}$ [29].

3.6. Bi-refringence measurements on quenched PC sheets

Quenching experiments were carried out on Bayer "Makrolon" polycarbonate sheets of thickness 1.09, 3.23 and 6.09 mm. This range of sheet thickness was investigated in order to obtain a significant range of Biot modulus in the quenching experiments. Sheets of 80 mm by 80 mm were dried at 120° C for 24h, then heated to 170° C for more than 1 h to allow any molecular orientation to relax. The sheets were quenched into iced water, then a strip of width in the range 3 to 6 mm was cut using a Metallurgical Services high speed abrasive wheel cut-off machine. The cut surfaces were polished using SiC papers, and 5 μm and 0.1 μm alumina paste. The strip was then placed between circularly polarizing filters, and photographed using a camera with close up rings, or a low powered microscope. The light path was in the x-direction of Fig. 2a, and either a sodium vapour lamp (wavelength 0.589 μm) or white light was used to find the zero order isochromatic fringe. In the central part of these strips the isochromatic fringes were all parallel to the sheet surfaces.

Slices of thickness less than 20% of the sheet thickness were then cut from these strips using a Buehler 'Isomet' low speed diamond saw, with water plus detergent as a cutting fluid. The slicing plane was normal to the length of the strip. The bi-refringence variation across these slices was again measured, with the light path in the x-direction of Fig. 3, using a Babinet Compensator. The orientational bi-refringence found in these slices varied in the same manner as did the total bi-refringence found in the long strips, except that its magnitude was 10 to 20% of the total bi-refringence.

The orientational bi-refringence found in the thin slices was plotted against the z-co-ordinate, and then subtracted from a similar plot of the bi-refringence in the strip against z. The result is the bi-refringence due to the residual stresses. Equation 15 was then used to find the principal stress difference, using a value of 78×10^{-12}

$m^2\,N^{-1}$ for the stress optical coefficient of Makrolon polycarbonate [30], a value that has been checked in these laboratories. The principal stress, σ_{zz}, perpendicular to the sheet surface was found to be zero, by the analysis that leads to Fig. 12, so the values of σ_{yy} (z), the residual stress distribution in the sheet $(= \sigma_{xx}\,(z)$ by symmetry), are obtained. Fig. 11 shows these residual stress distributions. They are slightly in error because the average of σ_{yy} across the section is not zero, the average values of σ_{yy} being $-2.4\,MN\,m^{-2}$ for the 1.09 mm sheet, $+0.5\,MN\,m^{-2}$ for the 3.23 mm sheet, and $+2.2\,MN\,m^{-2}$ for the 6.09 mm sheet. The 1.09 mm sheet had an orientational bi-refringence that clearly varied with position, so errors of this magnitude were expected to arise. Table V compares the surface and central residual stresses from Fig. 11, with the predicted residual stresses from the finite difference model for a range of heat transfer coefficients.

It is clear from Table V that using a heat transfer coefficient of $200\,W\,m^{-2}\,K$ results in predicted residual stresses that are too low, and that vary too much with sheet thickness. A heat transfer coefficient of $1000\,W\,m^{-2}\,K$ produces the correct magnitude of residual stresses, but again these vary too much with sheet thickness, whereas when $h = 4000$ the central residual stresses are suitably thickness independent, but the predicted surface residual stresses are too high and too variable.

In order to check the validity of the predicted effects of sectioning a residually stressed sheet, a thick slice, of square cross-section, from a 6.15 mm PC sheet quenched from 160 to 0° C was examined between circularly polarized sodium light. Luckily, in this sheet, the orientational bi-refringence observed in a thin slice was independent of the z-co-ordinate, so isochromatic fringes shown in Fig. 13b are contours of maximum shear stress, and they have been labelled with the shear stress values. Comparing Fig. 13a and b it is clear that the overall patterns are similar in shape and magnitude, with the compressive stress maxima occuring at the midfaces, and that there is a balanced biaxial stress state at the centre of the specimen. There are differences in the shapes of the lower contour levels but these do not invalidate the main features of the analysis.

4. Discussion

Having modified the analytical theory of Aggarwala and Saibel [8] so that both the Young's modulus and the thermal diffusivity of the polymer were temperature dependent it was rather surprising to see how little effect this had on the shape and magnitude of the residual stress distribution. However, the finite difference one-dimensional cooling calculation is easy to implement, and is certainly no more complex than the integrals in the theory of Aggarwala, especially when further terms are required for high values of the Biot modulus. It is clear that, in order to be able to predict the residual stresses arising from sheet quenching experiments, reliable values of the heat transfer coefficient are essential. The value for the quenching of polycarbonate in iced water has been found both from analysing cooling curves, and from comparing the predicted and actual residual stresses for different sheet thicknesses. This latter

TABLE VA Surface residual stresses in polycarbonate sheets quenched from 170 to 0° C

Sheet thickness (mm)	Surface Residual Stress MN m^{-2}			
	Experimental value	$h^* = 200$	$h = 1000$	$h = 4000$
1.09	−24.0	− 5.2	−16.3	−32.5
3.23	−21.0	−11.5	−28.3	−44.8
6.09	−23.6	−17.2	−36.0	−50.2

*h in W m^{-2} K.

TABLE VB Central residual stresses in polycarbonate sheet quenched from 170 to 0° C

Sheet thickness (mm)	Central Residual Stress MN m^{-2}			
	Experimental value	$h^* = 200$	$h = 1000$	$h = 4000$
1.09	4.0	2.4	7.0	10.4
3.23	7.0	5.1	9.8	11.4
6.09	10.0	7.2	10.8	11.7

*h in W m^{-2} K.

method has been used successfully for soda-lime glass sheets [31]. Although the agreement between theory and experiment is not exact, it is clear that the heat transfer coefficient is in the range 1000 to 4000 $W m^{-2} K$. These values can be compared with the value calculated for a vertical plate of height 80 mm from the properties of water, using the Grashof, Nusselt and Prandtl numbers [17], giving 830 $W m^{-2} K$.

The value of 2 $W m^{-2} K$ calculated by Saffell and Windle (or 200 $W m^{-2} K$ when the numerical error is corrected) is too low, the reason being that the cooling curve of the centre of a sheet is insensitive to the heat transfer coefficient, once it exceeds $\sim$ 1000 $W m^{-2} K$, as Fig. 7 shows.

Calculations of the effect of sectioning a residually stressed plate validate the experimental approach of Saffell and Windle [2]. It is clear that the slice thickness must be less than 20% of the sheet thickness for residual stresses to be reduced to $< 5\%$ of the initial values. However, the details of the stress distribution in a section of thickness equal to the sheet thickness, or near the end of a long strip, could not easily be guessed. Again it is not easy to guess the effect of partially cutting through a residually stressed sheet; Fig. 14 shows that the residual stresses act to close a crack even when it has grown into the region of the sheet that was initially under tension.

For the approach reported here to be of more general use it must be extended to two-dimensional heat flow, and to processes where pressure variation and material flow occur during soldification. A start has been made by Rigdahl [13] who analysed the heat flow in an injection mould cavity of size 50 mm by 50 mm by 5 mm. He assumed that the temperature of the polystyrene in the cavity was constant in the z (thickness) direction, and that the heat transfer coefficient to the mould wall was 150 $W m^{-2} K$ (The Biot modulus for heat flow in the thickness direction is 1.9, which shows that there will in fact be significant temperature gradients in this direction). He used a standard method to calculate the time dependent temperature distribution $T_{(x,y)}$, and predicted that a solid skin would form at the periphery of the moulding and grow in towards its centre. It is not clear what assumptions he made to calculate the "equivalent temperature loads" from the temperature distribution, particularly as polystyrene above T_g was taken to be an elastic solid, nor was it stated whether the cavity pressure of 100 $MN m^{-2}$ stayed constant with time. Consequently the results of his finite element analysis are of limited value. They can show that there is a residual compressive stress of between -12 and -20 $MN m^{-2}$ around the outer 50 mm by 50 mm perimeter, and that the residual tensile stress in the central region is < 2 $MN m^{-2}$. A simple calculation of the residual stresses arising from heat flow in the z-direction in the central part of the plate using Fig. 5 shows that the surface stress is -13 $MN m^{-2}$ and the midplane stress is 5 $MN m^{-2}$ for the same heat transfer conditions that Rigdahl used. Therefore the residual stress distribution will be more complex than the one he describes. Nonetheless this finite element calculation is far superior to the assumption, as in Reference [31], that the residual stresses due to two-dimensional heat flow are a linear superposition of those due to the one dimensional components of heat flow on their own. It should now be possible to develop a better theory of the residual stresses as a result of two-dimensional heat flows in injection mouldings, using information from cavity pressure transducers to provide realistic data on the feeding of the mould.

The analysis presented here has neglected the known viscoelastic behaviour of glassy polymers in the temperature range near T_g. This has not lead to serious errors in predicting the residual stress levels in sheets that have been cooled rapidly through this temperature range, but the analysis might be more in error for more slowly cooled sheets. Lee *et al.* [32] have shown how to use a thermorheologically simple viscoelastic model in calculating the residual stresses in tempered silicate glasses, and it should be possible to use a similar approach for polymeric glasses.

Turning to the use of quenching to modify the properties of plastics, [33] it is evident from the foregoing analysis that the disparate aims of either inducing residual stresses, or producing a glass with as low a density as possible, are capable of separate achievement. To obtain high residual stresses the requirements are a high Biot modulus, and as low a temperature for the quenching bath as possible. Thus thick sheets, and a high heat transfer coefficient to a liquid medium are desirable, but there is no need to heat the polymer to more than about $T_g + 20$ deg. However, there is a limit to the level of residual stresses that can be achieved. Not only does the compressive yield of the polymer set an

upper limit, but also the process of stress relaxation sets in at about 50% of the yield stress for PC, as shown by Yannas and Doyle [34]. Consequently for PC the upper limit on the surface compressive stress is about 30 MN m^{-2}. If a glassy polymer is required to be quenched so that it is as far as possible from its equilibrium glassy state, and yet contain no significant residual stresses, it should be quenched to a temperature roughly 20° C below the solidification temperature, i.e. to 120° C for PC, and then, when the temperature has equilibrated in the glassy state after the order of 1 minute, it should be cooled to room temperature. A similar cooling history is recommended for PC injection mouldings, presumably to minimize residual stresses and molecular orientation.

The effect of residual stresses in glassy polymers are by no means so beneficial as they are in soda-lime–silica glasses. This is because of the lower magnitude of the potential residual stress, for polymers having low solidification temperatures. and because of the stress relaxation process that can occur subsequent to quenching. Moreover such residual stresses can be potentially harmful, as can be shown by drilling a hole through a residually stressed PC sheet (as is done to provide the chin strap fixing point is some motor-cycle safety helmets) then exposing the hole to a stress crazing agent. The ductility of PC allows the drilling of holes, and yet with the stress concentration factor of 2 for a circular hole in a biaxially stressed sheet, it is not surprising that crazes develop at the mid thickness of the sheet, around the perimeter of the hole.

Acknowledgements

I am grateful to Mr. R. Greenway for making some of his project results available.

References

1. P. SO and L. J. BROUTMAN, *Polymer Eng. Sci.* **16** (1976) 785.
2. J. R. SAFFELL and A. H. WINDLE, *J. Appl. Polymer Sci.* **25** (1980) 1117.
3. G. J. SANDILANDS and J. R. WHITE, *Polymer* **21** (1980) 338.
4. L. D. COXON and J. R. WHITE, *J. Mater. Sci.* **14** (1979) 1114.
5. *Idem, Polymer Eng. Sci.* **20** (1980) 230.
6. D. P. RUSSELL and P. W. R. BEAUMONT, *J. Mater. Sci* **15** (1980) 197.
7. A. I. ISAYEV and C. A. HIEBER, *Rheol. Acta.* **19** (1980) 168.
8. B. D. AGGARWALA and E. SAIBEL, *Phys. Chem. Glasses* **2** (1961) 137.
9. R. GARDON, in "Glass: Science and Technology" Vol. 5, Edited by D. R. Uhlmann and N. J. Kriedl (Academic Press, New York, 1980).
10. J. KUBAT and M. RIGDAHL, *Int. J. Polymer Mater.* **3** (1975) 287.
11. W. KNAPPE, *Kunstoffe* **51** (1961) 562.
12. S. TIMOSHENKO and J. N. GOODIER, "Theory of Elasticity", 2nd Edition, (McGraw Hill Book Co., New York, 1951).
13. M. RIGDAHL, *Int. J. Polymer Mater.* **5** (1976) 43.
14. N. J. MILLS, *J. Mater. Sci.* **16** (1981) 1317.
15. B. S. THAKKAR, L. J. BROUTMAN and S. KALPAKJIAN, *Polmer Eng. Sci.* **20** (1980) 756.
16. H. S. CARSLAW and J. C. JAEGER, "Conduction of heat in solids" 2nd Edition (Oxford University Press, London 1959).
17. A. J. CHAPMAN, "Heat Transfer", 2nd Edition (MacMillan, New York, 1967).
18. R. GARDON, *J. Amer. Ceram. Soc.* **41** (1958) 200.
19. S. KENIG and M. R. KAMAL, *SPE Journal* **26** (1970) 50.
20. O. S. NARAYANASWAMY, *J. Amer. Ceram. Soc.* **61** (1978) 146.
21. H. ABEN, "Integrated photoelasticity", (McGraw Hill Book Co., New York, 1979).
22. R. BERLOT, *Plast. Mod. Elast.* **18** (1966) 231.
23. K. H. HELLWEGE, W. KNAPPE and P. LEHMANN, *Kolloid. ZZP* **183** (1962) 110.
24. J. M. O'REILLY, F. E. KARASZ and H. E. BAIR, *J. Polymer Sci. C.* **6** (1963) 109.
25. K. EIERMANN, *Kunstoffe*, **55** (1965) 335.
26. R. GREENWAY, Birmingham University, Unpublished work (1981).
27. D. HANDS, *Rubber Chem. Technol.* **50** (1977) 480.
28. W. R. KRIGBAUM, *J. Polymer Sci.* **15C** (1966) 251.
29. J. A. MANSON and R. W. HERTZBERG, *C.R.C. Crit. Rev. Macromol. Sci.* **1** (1975) 433.
30. A. KUSKE and G. ROBERTSON, "Photoelastic Stress Analysis", (Wiley, London, 1974).
31. N. K. SINHA, *Proc. Soc. Exptl. Stress Anal.* **35** (1978) 25.
32. E. H. LEE, T. G. ROGERS and T. C. WOO, *J. Amer. Ceram. Soc.* **48** (1965) 480.
33. N. J. MILLS, *J. Mater. Sci.* **11** (1976) 363.
34. I. V. YANNAS and M. J. DOYLE, *J. Polymer Sci. A2* **10** (1972) 159.

Received 22 May
and accepted 15 July 1981